applied sciences

MDPI

Article

VIS-Light-Induced Degradation of Street Art Paints and Organic Pigments

Nicolò Guarnieri [1], Claudia Conti [2], Matteo Passoni [3], Kevin Ambrogioni [3], Paulina Guzmán García Lascurain [1], Sara Goidanich [1,*] and Lucia Toniolo [1]

[1] Dipartimento di Chimica, Materiali e Ingegneria Chimica "G. Natta", Politecnico di Milano, 20133 Milan, Italy
[2] Institute of Heritage Science (ISPC), National Research Council (CNR), 20125 Milan, Italy
[3] Dipartimento di Energia, Politecnico di Milano, 20156 Milan, Italy
* Correspondence: sara.goidanich@polimi.it

Abstract

Contemporary murals are highly susceptible to rapid color fading due to outdoor urban exposure. This study investigates the photodegradation mechanisms affecting synthetic organic pigments (SOPs) and commercial acrylic–vinyl paints under simulated visible light exposure. Artificial aging experiments were conducted on two types of systems: (*a*) pigment pellets, composed of pre-fixed pigments on mineral bases, as supplied by the manufacturer, and (*b*) commercial paints applied on glass substrates. Both systems were aged under controlled and uncontrolled relative humidity (RH) conditions. Colorimetric analyses revealed significant color fading, particularly in pigments PR112, PO5, and PV23. Vibrational spectroscopies highlighted the reduction in pigment-related bands after aging, indicating SOPs' vulnerability to photodegradation. In paint mock-ups, FTIR-ATR measurements indicated binder degradation and an increase in signals from inorganic fillers. A superficial layer enriched in inorganic components was investigated non-invasively by Micro Spatially Offset Raman spectroscopy (Micro-SORS) in the beamsteer modality. It highlighted a gradient of calcite to pigment with depth. These findings indicate that color fading in mural paints results from the combined degradation of both pigments and binders.

Keywords: color fading; photofading; street art; modern paints; Micro-SORS; light aging

Academic Editor: Alessandra Biancolillo

Received: 31 July 2025
Revised: 15 September 2025
Accepted: 16 September 2025
Published: 18 September 2025

Citation: Guarnieri, N.; Conti, C.; Passoni, M.; Ambrogioni, K.; Guzmán García Lascurain, P.; Goidanich, S.; Toniolo, L. VIS-Light-Induced Degradation of Street Art Paints and Organic Pigments. *Appl. Sci.* **2025**, *15*, 10188. https://doi.org/10.3390/app151810188

1. Introduction

Color fading in street art paintings has been described as a rapid phenomenon, influenced by solar radiation, the composition of the painting materials, substrate preparation, and environmental conditions, that refers specifically to an irreversible change in color induced by light irradiation and the photodegradation of materials [1,2]. As a result, the readability and appearance of some urban paintings can be compromised within just a few years. The increasing cultural and social importance of contemporary murals is raising questions to curators and conservators, and a need to develop adequate strategies for the preservation of these artworks in outdoor conditions [3].

Exposure to solar radiation has been identified as a primary factor contributing to the deterioration of materials, resulting in color fading [4–8]. Together, the relative humidity and temperature can influence the photodegradation of polymer matrices [2,7,9]. A high relative humidity can significantly accelerate photodegradation processes, especially in porous substrates, by enhancing moisture diffusion and facilitating oxygen penetration [2].

However, the extent of RH influence is highly dependent on the chemical nature of the dye and the substrate [2]. In some cases, rapid color fading was reported shortly after the creation of the artwork [4,9,10]. Moreover, a clear association was observed in the literature between the chemical composition of the paint mixture, the substrate, and the rate at which it fades [1,5,11,12]. Previous research [4] has suggested that specific ingredients of the paint mixture (e.g., some specific pigments) can be particularly susceptible to photochemical instability, which results in significant color changes. The same study also demonstrated that fading could affect less than 10 μm of the paint surface. The photodegradation of the binder leads to pigment loss and the surface enrichment of white fillers. This process leads to the so-called chalking effect, which contributes to the perceived color change [4,6,9,13].

Solar radiation, particularly its ultraviolet (UV) component, plays a key role in the degradation of organic compounds through a process known as photodegradation. When exposed to sunlight, colorants within the polymer matrix absorb photons, leading to the generation of free radicals. These radicals react with oxygen, breaking polymer chains and lowering the molecular weight. This degradation process leads to visible and mechanical deterioration such as discoloration, embrittlement, and the loss of gloss. It has been reported that, while both UV and VIS light can induce the photodegradation of organic dyes [2,14], the visible region plays a predominant role in the color fading of azo compounds [14]. The higher sensitivity of azo dyes to visible light is attributed to their specific chemical structure, which enables efficient absorption in this spectral region and facilitates degradation pathways even at photon energies lower than the UV range.

Synthetic organic pigments (SOPs) have been extensively studied for their light-induced aging behavior under simulated outdoor conditions. Research has shown that the photostability of SOPs is primarily influenced by their chemical structure and their interaction with the surrounding matrix. Anghelone et al. [15] demonstrated that, while SOP powders (naphthol AS, diketopyrrolopyrrole, and quinacridone) exhibited stability under simulated solar exposure, the aging effects affected more the alkyd and acrylic binders of paints. Further, certain pigments [2,16,17] can act as photosensitizers, accelerating binder degradation by acting as light absorbers or photochemical initiators. Similarly, Marazioti et al. [7] suggest that light aging tends to affect polymeric binders more significantly than organic pigments and inorganic fillers. As a consequence, the degradation or loss of the binder leaves the pigments more exposed to radiation, thereby increasing their vulnerability to further photodegradation [5].

The use of the naphthol AS pigment in street art has been documented in the literature [18–21], and its instability has been confirmed in case studies conducted in various climatic conditions [4,22–24], as well as in previous mock-up accelerated aging experiments [8,15,25–27]. The current literature confirms that light radiation is the primary agent of degradation in SOP-based paints, with binder degradation reported as a major contributing factor. In contrast, the role of humidity is less frequently considered.

For these reasons, the objective of this study is to investigate the mechanisms responsible for color fading in acrylic–vinyl paints, which were previously identified as particularly susceptible to fading in different case studies [5,24]. The research focuses on isolating and evaluating, with a multi-technique analysis, the roles of SOPs and binders under controlled VIS-light and RH conditions.

To gain a comprehensive understanding of the fading mechanisms, a dual experimental approach was adopted, involving both pigment pellets and commercial paint mock-ups. This strategy facilitates isolating and evaluating the contributions of the two components (SOPs and binders) to the observed chromatic changes. The core aim of this study is to determine whether color fading is primarily driven by the photodegradation of the binder

(potentially leading to the detachment or loss of pigmented particles) or by the intrinsic photochemical instability of the SOPs themselves.

In addition, this study aims to clarify the role of relative humidity (RH) in photodegradation processes. Particular attention is given to the potential synergistic effects between VIS light exposure and RH conditions, an aspect that remains mainly underexplored in the current literature. Indeed, most of the existing studies focus either on pigment or only binder degradation, under UV exposure. This leaves a gap in understanding how VIS-light and RH jointly influence the deterioration of SOPs and complete paint systems in outdoor environments. In actuality, the radiation acting on contemporary murals exposed to solar radiation is largely composed of visible light, which represents the main portion of the spectrum directly interacting with pigment molecules: it is, therefore, dramatically important to state how this condition affects the conservation of painted surfaces.

To this end, a custom-built light aging chamber was employed to simulate visible light aging. During irradiation, the samples were also subjected to two environmental conditions, a high relative humidity and an uncontrolled ambient RH, in order to assess the influence of moisture and the potential synergistic interaction with VIS light. The degradation processes were monitored through a multi-technique approach combining reflectance VIS, ATR-FTIR, and Micro-SORS spectroscopies. This integrated strategy is essential when studying complex formulations, as it enhances the reliability of the analysis and enables a more comprehensive understanding of material transformations.

2. Materials and Methods

2.1. Sample Preparation

Artificial aging experiments were conducted on two types of model systems: (*a*) a simplified system composed of pure pigment pellets, prepared using pigments that are pre-fixed on mineral bases (calcite and/or gypsum) as provided by the manufacturer, to investigate the degradation mechanisms affecting selected SOPs; and (*b*) a more complex system consisting of commercial paints made of a binder, pigments, and inorganic fillers. Pigment pellets (diameter 1.2 cm) were prepared by compressing the dry pigment powders (Kremer pigmente GmbH & Co. KG, Aichstetten, Germany) into uniform pellets using a hydraulic press. Commercial paints (VIP Professional 08, J Colors S.p.a., Italy) were applied onto glass microscope slides using a manual doctor blade procedure to ensure consistent layer thickness and surface coverage. Two paint formulations were selected, both sharing the same binder and fillers composition, and containing two of the pigments that showed the most relevant color fading. Details of the material involved in the experiment are provided in Table 1. Alizarine Crimson Light (23600, Pigment Red 112, C.I. 12370, Kremer pigmente GmbH & Co. KG, Aichstetten, Germany) was used as reference of pure pigment powder for collecting reference FTIR spectra.

Table 1. List of commercial paints and pigments involved in the study, including their chemical composition and constitutive index (C.I) designation of the contained pigments.

Name	Type	Composition	C.I. Pigment
Red paint	Paint on glass slide	Acrylic vinyl binder + calcite + kaolinite + PR112	Naphthol Red AS-D C.I. 12370
Orange paint	Paint on glass slide	Acrylic vinyl binder + calcite + kaolinite + PO5	Hansa Orange RN C.I. 12075
PR112 55400	Pigment pellet	PR112 + $CaCO_3$	Naphthol Red AS-D C.I. 12370
PR112 55300	Pigment pellet	PR112 + $CaCO_3$ + $CaSO_4 \cdot 2H_2O$	Naphthol Red AS-D C.I. 12370
PO5 55200	Pigment pellet	PO5 + $CaCO_3$	Hansa Orange RN C.I. 12075
PY83 55125	Pigment pellet	PY83 + $CaCO_3$	Diarylide Yellow HR C.I. 21108
PY74 55100	Pigment pellet	PY74 + $CaCO_3$	Arylide Yellow 5GX C.I. 11741
PV23 55900	Pigment pellet	PV23 + $CaCO_3$	Dioxazine Violet C.I. 51319

2.2. Light Aging

Artificial aging was carried out using a custom-built light chamber, equipped with photographic spiral compact fluorescent light bulbs (CFLs). The radiation spectrum was limited to visible light in order to simulate mild accelerated aging, and obtain a better follow-up of the color fading. The chamber, measuring 70 × 40 cm, is constituted by wooden walls internally lined with reflective aluminium sheets (food-grade). Illumination was provided by seven cold spiral CFL bulbs (Walimex pro, 125 W, spiral CFL, 5500 K, 5600 lumen) delivering homogeneous visible light at a color temperature of 5500 K and a total illuminance of 50 ± 11 klux (emission spectrum in Supplementary Figure S1). Mock-ups were aged horizontally under two different environmental conditions to assess the role of relative humidity: one set was exposed to VIS-light under controlled high relative humidity (RH), maintained constant throughout the exposure period using a saturated KNO_3 solution; the second set was exposed to the same light conditions but without RH control, under ambient variable laboratory humidity. This setup allowed the investigation of the combined and individual effects of visible light and RH on the aesthetic, chemical, and physical stability of the model paint and pigments systems. Although the temperature inside the chamber was not actively controlled, it was regularly monitored during all the duration of the experiment (33.8 ± 5.2 °C). The use of saturated salt solutions such as KNO_3 is a well-established method for maintaining stable RH environments, with tabulated values available across a range of temperatures. According to literature [28], saturated KNO_3 solutions consistently maintain RH values around 85% and 90% under measured temperatures. Periodic RH and temperature checks confirmed the environmental conditions, with values recorded in aging environments (aging chamber without RH control and chamber with high RH) as reported in Table 2. The aging process was conducted over a period of 100 days, under continuous exposure (24/7). The simulated light aging conditions corresponded to approximately 1.6 years of natural horizontal exposure or to about 7 years of vertical orientation exposure in Milan, Italy [29,30]. The use of an in-house light aging chamber provided flexibility in modulating the total power of illuminance (adjusting the number of the bulbs), adapting the size of the chamber to the set of samples and controlling simultaneously different environmental conditions (i.e., RH levels through sealed desiccator containing a saturated solution), within a single experimental setup. Additionally, the system allowed for cost-effective operation, as the light sources could be easily replaced using commercially available CFL bulbs.

Table 2. Mean and standard deviation values of relative humidity (RH) and temperature (T) recorded in experimental environments used during artificial aging tests, compared to the laboratory conditions.

Environment	RH Mean (%) ± SD	T Mean (°C) ± SD
Light chamber without RH control	41.2 ± 5.9	35.6 ± 3.0
Light chamber at high RH environment	80.5 ± 11.5	33.8 ± 5.2
Laboratory environment	67.4 ± 0.9	24.5 ± 1.4

It should be emphasized that the aging process was intentionally designed to isolate the effects of visible (VIS) light irradiation and relative humidity (RH), while excluding other environmental factors typically present in natural outdoor exposure (i.e., erosion, temperature fluctuations, pollutants, and rainfall). To provide a comparative reference, natural aging was also conducted by exposing paint mock-ups to outdoor conditions on a south-facing window in an urban setting (Milan, Italy). This natural exposure lasted 210 days and was divided into two spring–summer intervals: the first from July to September 2023, and the second from March to September 2024. These periods were specifically chosen to avoid excessive rainfall and humidity. It has to be underlined that, in general,

establishing a direct equivalence between natural and artificial aging is inherently challenging; therefore, the natural aging data were used mainly for comparative purposes and to represent a multifactorial outdoor exposure scenario in Milan, Italy.

2.3. Methods

Optical microscopy (Leica DM6 3D, Leica Microsystems, Milan, Italy with an objective of 20×–50×, and LASX software 5.1.0.25593) was used to assess the surface morphology.

Temperature and relative humidity (RH) were periodically monitored using a Testo 175 H1 data logger (Testo S.p.a., Settimo Milanese, Italy), while illuminance was verified using a luxmeter (ISO-TECH ILM 1335 Light Meter, Isotech, RS Components S.r.l., Sesto San Giovanni, Italy).

VIS reflectance spectroscopy (Spectro-colorimeter CM-2600d Konica Minolta, Tokyo, Japan; D65 light source at 10°, spot size of 8 mm) evaluated color fading after aging by collecting 10 measurements per mock-up paints. CIELab color space were used to elaborate the measurements and calculate ΔE_{ab} values [31,32]. ΔE values obtained under high and laboratory RH conditions were compared using independent two-sample *t*-tests.

In the case of pigment pellets, due to the limited aperture size of the reflectance spectrophotometer, direct colorimetric measurements via VIS reflectance spectroscopy could not be performed. For this reason, color changes of SOP pellets were assessed through calibrated photographic imaging. Images were acquired using a Nikon D750 camera (Nikon Corporation, Tokyo, Japan), equipped with Nikon AF-S 24–85 mm f/3.5–4.5 G ED VR lens, in combination with a Calibrite ColorChecker Passport for color calibration (Calibrite PROFILER software v.2.0). HEX color codes and L*, a*, and b* coordinates were extracted using Adobe Photoshop (Adobe Inc., San Jose, CA, USA, v.26.10), averaging the color selection within a 30×30-pixel area. To ensure a reliable comparison, aged pellets and a non-aged reference pellet were always photographed within the same calibrated image. Only ΔE values between samples in the same image were evaluated. This approach minimized variability due to lighting, camera settings, or calibration and improved the accuracy of color difference estimations. To assess the reliability of color difference measurements derived from calibrated digital images, we conducted a comparative analysis between this method and direct measurement using a VIS reflectance spectroscopy (described above). Comparative analysis (reported in Supplementary Materials Table S1) showed a strong correlation between the two methods, with ΔE discrepancies generally within acceptable tolerances. The Pearson correlation coefficient between the two datasets was R = 0.998, indicating a strong linear relationship. This result confirms that the image-based method closely mirrors ΔE measurements carried out with VIS reflectance equipment, supporting its use as a reliable and non-invasive alternative for color difference analysis.

μ-FTIR spectroscopy (Thermo Nicolet iN10 MX, Thermo Fisher, 128 scans, resolution 4 cm^{-1}) was used to analyze the chemical changes in the pigment pellets before and after aging. Micro sampling was performed with a needle under the microscope to collect material from the faded surfaces of the pellets. The collected samples were analyzed in transmission mode using a diamond anvil cell (DAC). ATR-FTIR spectra (Thermo Nicolet iZ10, SmartX accessory, ThermoFisher Scientific Inc., Waltham, MA, USA were acquired at 32 scans and resolution of 4 cm^{-1} to monitor the chemical changes of paint mock-ups during the aging at specific intervals. Compositional changes were evaluated, using software Opus (Bruker Optik GmbH, Ettlingen, Germany, version 8.5). Specific bands' intensity ratios (N method of OPUS) were calculated for calcite out-of-plane bending of carbonate ion (875 cm^{-1}) [5], kaolinite Si-O stretching (1030 cm^{-1}) [21,33], binder carbonyl group (1740 cm^{-1}) [21,34], photodegradation products of the binder (due to the formation of unsaturations at 1635 cm^{-1}) [35,36], and Naphtol pigments (750 cm^{-1}) [37–39].

Micro-SORS measurements were carried out using a Renishaw InVia Qontor Raman prototype [40] (785 nm laser, 10 mW, 50× LWD objective, NA 0.5, ~1.9 µm spot size, 10 s and 10 accumulations) on red paint mock-ups and on pigment pellets whose pigments peaks were not detected through FTIR spectroscopy. Spatial offsets (0, 3, 5, 7, 10, and 12 µm) were introduced using the beam-steering system, which is normally used to optimize the overlap of the laser illumination area with the Raman collection area on the sample surface for maximizing Raman signal. Here, this system is used to shift the laser spot across the sample surface via motorized mirrors, decoupling the excitation and collection zones, guaranteeing very small offset values, allowing the investigation of very thin depths [41]. Raman intensity ratios between the calcite (1085 cm^{-1}) [42] and the PR112 pigment peak (1110 cm^{-1}) [43,44] were evaluated based on the fitted peak heights, in order to monitor depth-dependent compositional changes. Six replica series were acquired both on aged and unaged mockups. Spectra were processed and fitted using an automated algorithm developed in Python (v.3.12). The statistics-sensitive non-linear iterative peak-clipping baseline correction is used after an adaptive smoothing of the spectra. The fitting procedure is then applied to the baseline-corrected spectra in two steps: the first using the differential evolution algorithm, stable to local minima of the objective function [45], and the second using a trust region algorithm to estimate the error on the parameters.

3. Results and Discussion

This section provides a concise and precise description of the experimental results obtained for the SOP pellets (§ 3.1) and for the mock-up paints (§ 3.2), aimed at clarifying the respective roles of RH, pigments, and binders in the observed degradation.

3.1. Pigments Pellets

Artificial aging experiments conducted on simplified systems composed of pigment pellets revealed that several SOPs are intrinsically prone to color fading when exposed to visible light. Significant color changes were observed for the tested pigment pellets after light aging (Table 3). Among them, PV23 and PR112 exhibited the most pronounced fading. Under high relative humidity (RH), PV23 showed an exceptionally high ΔE value of 76.2, indicating extreme fading and a near-complete loss of visual identity, as clearly documented in the photographic images (Figure 1). The corresponding shifts in a* and b* values reflect a transition from a violet-blue tone to a dull, whitish color. Even under uncontrolled ambient RH conditions, PV23 exhibited a substantial ΔE of 63.8, confirming its pronounced instability under light exposure regardless of humidity control. The red PR112 pigment showed severe chromatic shifts, with ΔE values reaching 19.8 when calcite is present and 16.7 when both calcite and gypsum are the mineral bases, indicating a significant color fading. Notable color variation was also observed for PO5, with ΔE values up to 9.9 under high RH, suggesting that elevated humidity may enhance the fading process. Overall, the results indicate that constant high relative humidity accelerates and intensifies color fading for PR112, PO5, and PV23.

The yellow pigments PY74 and PY83 also underwent a noticeable color fading process, with ΔE values ranging from 6.1 to 9.0. Although these values are lower than those recorded for PR112 and PV23, they are not negligible (higher than 3.5 units) and indicate perceptible alterations in chromatic appearance. Interestingly, the effect of constant high relative humidity (RH) differed from that observed in the previously described materials, resulting in a slower rate of color fading. This suggests that the influence of RH on pigment stability may vary depending on the specific pigment chemistry and formulation.

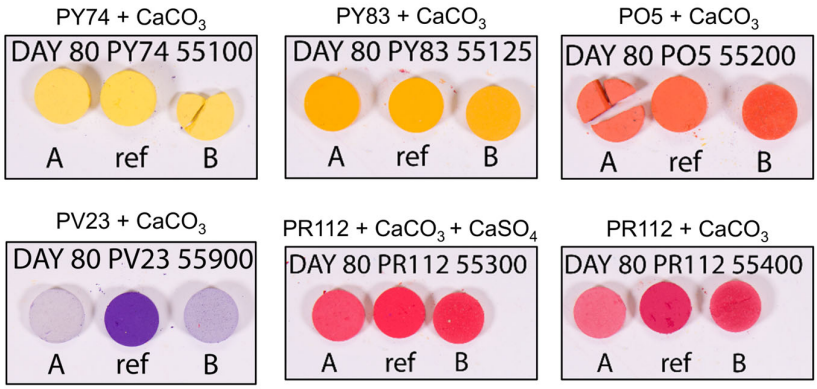

Figure 1. Calibrated photography images of the unaged (ref) and aged pigments pellets exposed to high relative humidity (RH: A) and uncontrolled environment (no control RH: B). All samples were photographed simultaneously within the same calibrated image to ensure consistent lighting and improve the reliability of color comparison.

Table 3. Colorimetric data (HEX codes, and L*, a*, and b* values) extracted from calibrated images of the pigment pellets. Unaged reference values are reported for each pigment to calculate ΔE differences with aged pellets (80 days) for environment A, with a constant high RH, and environment B, without the control of RH. Color data were extracted from a single calibrated image containing all three samples, in order to enhance the reliability of color comparisons.

	Ref Unaged				**Env. A: High RH**					**Env. B: No Control RH**				
	L*	**a***	**b***	**HEX**	**L***	**a***	**b***	**HEX**	**ΔE_A**	**L***	**a***	**b***	**HEX**	**ΔE_B**
PR112 55400	52	71	18	D54164	64	56	13	E67489	**19.8**	53	70	26	D7455C	**8.1**
PR112 55300	57	77	35	EC4558	60	67	22	E95C71	**16.7**	56	74	34	E54656	**3.3**
PO5 55200	67	59	50	F87857	66	55	41	F07B62	**9.9**	61	64	52	EC6146	**8.1**
PY83 55125	80	26	89	FFB735	79	28	88	FEB334	**2.4**	80	25	81	FFB844	**8.1**
PY74 55100	89	7	67	FFDB6F	89	8	61	FED979	**6.1**	89	7	58	FEDA7D	**9.0**
PV23 55900	35	44	−53	6936A3	82	8	−5	D4C7D4	**76.2**	74	12	−14	C0AFCD	**63.8**

Overall, the results confirm that the degradation of the tested synthetic organic pigments (SOPs) and the resulting color fading can occur independently of the binder matrix. These alterations are strongly influenced by the specific chemical composition of the pigments and the environmental conditions. The presence of the relative humidity (RH) appears to modulate the rate of degradation, although its effect is pigment-dependent.

The FTIR and Raman results are presented for representative pigment samples (PR112 and PV23), which exhibited the most pronounced changes. Nonetheless, FTIR analyses were performed on all pigment pellets, revealing consistent trends in the spectral modifications and degradation behavior. Microsamples were carefully collected from the outermost layers of the aged pellets (after 100 days of aging) and analyzed via FTIR, showing a significant loss of spectral features associated with the original pigments. Figure 2 illustrates the case of PR112 55300 as an example. Before aging, only few characteristic vibrational peaks of pigment PR112 can be detected, and only in spectral regions which are not dominated by calcite and gypsum signals. These peaks, highlighted with asterisks in Figure 2, significantly decreased in intensity after aging, particularly the band at 750 cm^{-1}, which disappeared in the spectrum of the faded pellet. This band may be attributed to the C-Cl stretching [37] or out-of-plane aromatic C–H bending [38,39]. From these ATR-FTIR results, it is not possible to assess if the observed loss of vibrational bands can be ascribed to a loss of pigment itself in the mixture, or if it should be ascribed to a photo-induced molecular modification. These findings, in any case, confirm that synthetic organic pigments

(SOPs) are susceptible to degradation when exposed to prolonged VIS light. Since earlier studies [15] have reported that PR112 remains stable under UV irradiation for up to four months of light aging, the present results make it possible to hypothesize that color fading is mainly due to the physical loss of pigment particles on the surface.

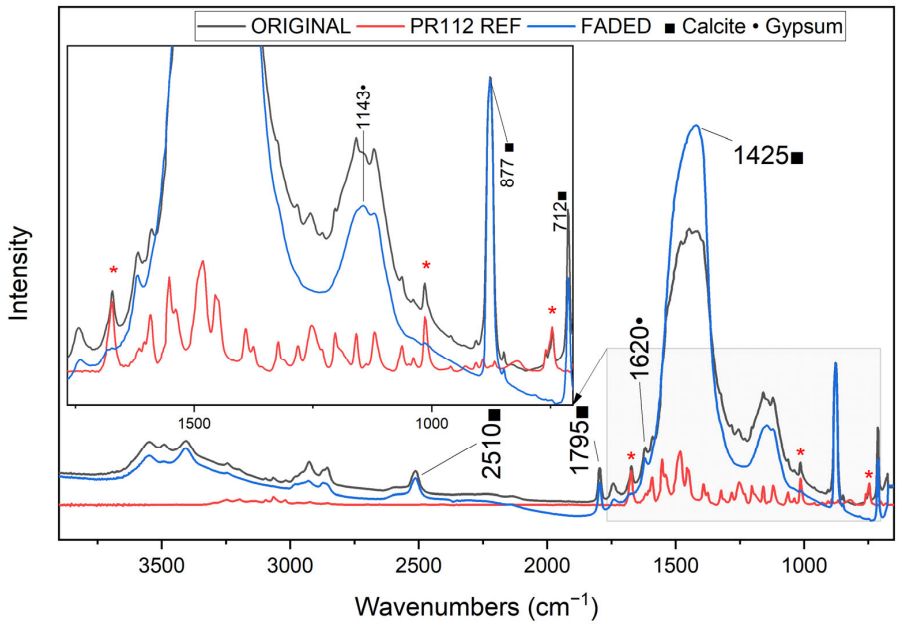

Figure 2. Transmission μ-FTIR spectra (DAC mode) of original (black) and faded (blue) PR112 55300 pigment pellet, alongside the reference PR112 spectrum (red). Characteristic bands of the pigment (red * asterisks) [46] are no longer visible in the aged sample. Peaks attributed to calcite (■) and gypsum (●) are assigned [47,48].

In the case of PV23 pellets, FTIR spectroscopy failed to detect any discernible pigment-related signals. However, Raman spectroscopy confirmed a strong decrease in pigment-related peaks (highlighted with purple asterisks in Figure 3 [49]), consistent with the colorimetric analyses (Table 3). Notably, Raman spectra of aged samples revealed a relative increase in the intensity of signals associated with inorganic components (anhydrous calcium sulfate, gypsum, and calcite). Additionally, spectral evidence suggests a transformation of gypsum into anhydrite in the faded spectra.

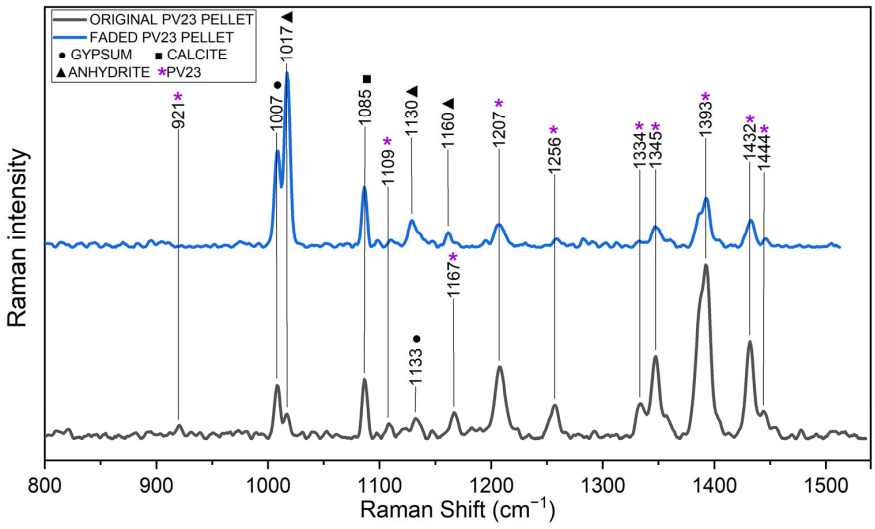

Figure 3. Raman spectra of original (black) and faded (blue) PV23 pigment pellets. A pronounced reduction in peaks related to PV23 (indicated with purple asterisks [49]) is evident in the aged spectrum.

Given that signals from the inorganic mineral phases dominate large regions of the IR and Raman spectra, and that pigment-related signals are significantly reduced in the spectra of the faded samples, it remains uncertain whether the pigment undergoes structural modifications, fragmentation, or conversion into other compounds during aging. The loss of the organic pigment (and the consequent relative enrichment of the inorganic filler) has been discussed in the literature [22] as a consequence of the local photodegradation of pigment molecules (PO34, Pigment Orange 34, in that specific literature case) via a photocatalytic mechanism. This process may lead to the formation of volatile species (e.g., H_2O and CO_2) that are released from the paint surface. Some degradation by-products of PR112 have been identified in the literature, which may alter its spectroscopic response and contribute to the observed signal loss [23]. While this mechanism appears to be a plausible explanation for the observed loss of pigment signals, the current FTIR data do not allow for a definitive confirmation. Further investigations are needed in order to better understand the degradation pathways of these pigments.

3.2. Commercial Paint Mock-Ups on Glass Slides

The artificial aging of commercial paint systems (composed of pigment, binder, and inorganic fillers) revealed clear evidence of color fading after 100 days of exposure to visible light. This is visually documented in Figure 4, which shows the appearance of aged mock-ups under different RH conditions. The aging was limited to two types of paints, both sharing the same chemical composition but containing different pigments: "Red" with PR112 and "Orange" with PO5. The progression of aging was monitored using periodic colorimetric and ATR-FTIR measurements (Figure 5). Similar to the pure pigment pellets, the red paints containing PR112 showed the most severe degradation, with ΔE values exceeding 10, indicating a significant color change. This confirms that the pigment is particularly vulnerable to color fading even within more complex paint formulations. Figure 5 also reports the colorimetric monitoring of natural aged paint mock-ups ("Red nat" and "Orange nat") and the control samples stored in the dark for an equivalent amount of time ("control").

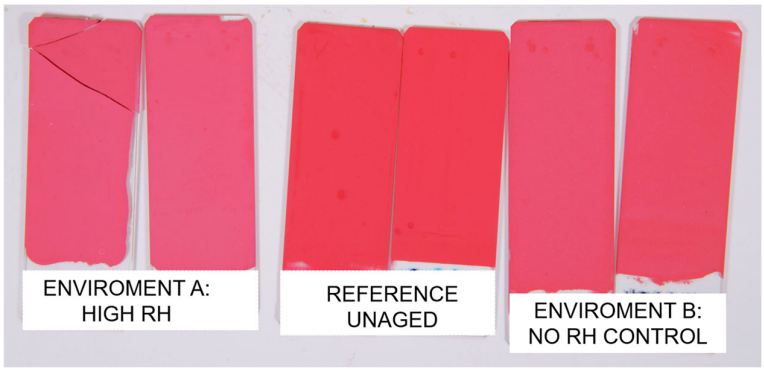

Figure 4. Calibrated photographs of the unaged (ref) and aged commercial paints mock-ups under RH (Environment A) and ambient RH without control (Environment B).

Moreover, also in this case, the role of relative humidity (RH) was found to be pigment-dependent. While a high humidity environment accelerated the fading of red paint, it had a minor effect on the orange one. This suggests that moisture may play distinct roles in the degradation of the pigment and binder, depending on their chemical nature and formulation. To statistically assess the pigment-dependent effect of RH on color fading, the ΔE values for red and orange paint mock-ups aged under high RH and uncontrolled conditions were compared. For the red paint, the mean ΔE under high RH was 11.13 ± 0.87, while, under an uncontrolled RH, it was 9.06 ± 0.28. The difference of 2.07 was statistically

significant (p = 0.0367). For the orange paint, the mean ΔE under high RH was 5.87 ± 0.40, while, under the uncontrolled RH, it was 6.92 ± 0.28. Although the difference between the values (1.05) is low, the statistical significance (p = 0.0226) confirms that RH has an impact on the color fading of this paint.

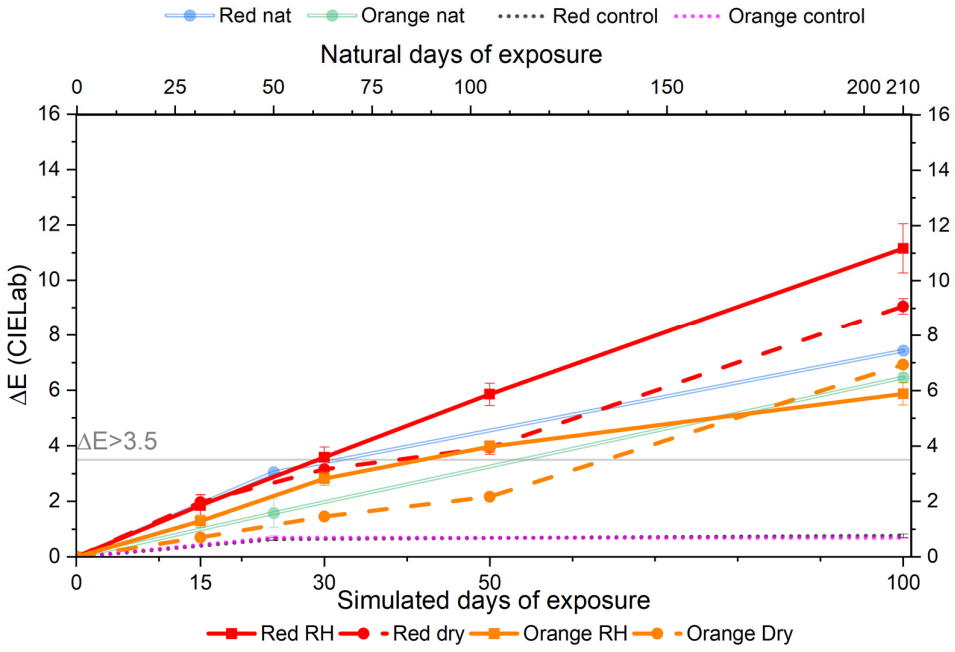

Figure 5. Evolution of ΔE values for red and orange paints mock-ups under the accelerated (bottom x-axis) and natural (top x-axis) light exposure. Solid lines represent high RH conditions; dashed lines indicate uncontrolled RH; and dotted lines show unexposed control samples. Note: artificial and natural aging are not directly equivalent.

High-magnification optical microscopy revealed the formation of white grains at the surfaces of the faded paint mock-ups, as shown in Figure 6b. Additionally, observation of the polished cross-sections identified the presence of a thin, superficial faded layer of paint (less than 10 µm of thickness) on top of the entire painting layer of approximately 200 µm (Figure 6c).

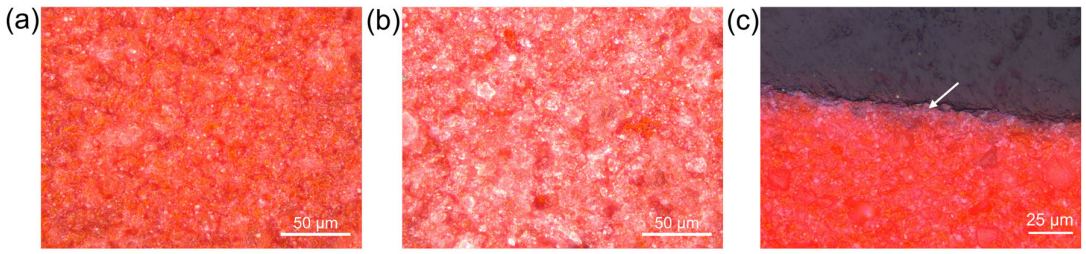

Figure 6. Optical microscopy images of red paint mock-ups at day 0 (**a**) and day 100 (**b**). (**c**) Cross section of the faded red paint mock-up (day 100) at 50×.

The chemical and molecular changes of the paint mock-ups were evaluated by collecting the ATR-FTIR spectra at regular intervals throughout the aging process. Principal Component Analysis (PCA) was applied to assess whether the technique could distinguish between the spectra of unaged and faded mock-ups. For the red paint, the PCA-scores plot (Figure 7a) shows a clear separation between the unaged samples (day 0) and those aged in a high relative humidity (RH) environment (red points). Notably, there is no overlap between the 90% confidence ellipses of the two groups, indicating effective differentiation.

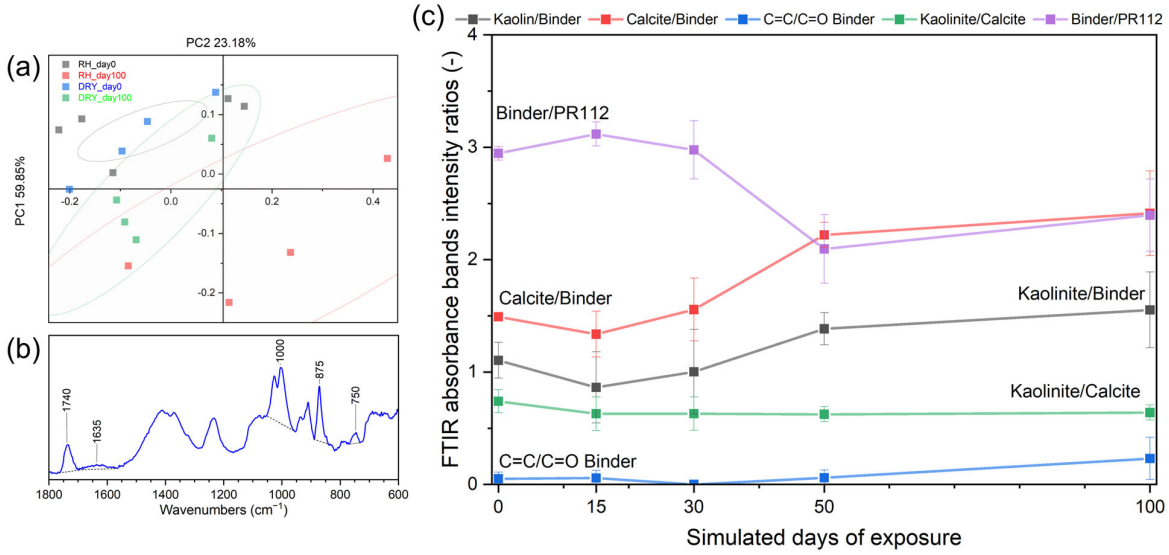

Figure 7. ATR-FTIR analyses of red paint mockups. (**a**) PCA scores plot at day 0 (RH: black, DRY: green) and day 100 (RH: red, DRY: blue), showing separation between unaged and aged samples under high RH conditions (ellipses indicate 90% confidences); (**b**) example of FTIR band intensity integration; and (**c**) evolution of ATR-FTIR bands' intensity ratios for red paint in high RH aging environment at 0, 15, 30, 50, and 100 days of simulated days of exposure: ratios related to inorganic fillers (black and red line) increase over time, bands associated with binder degradation increase (blue), and binder bands decrease slightly faster than the pigments (purple line).

The ATR-FTIR measurements (Figure 7b,c) revealed a marked decrease in the intensity of binder bands on aged surfaces, along with an increase in filler-related bands. As aging progressed, a systematic increase in the relative spectral contribution of inorganic fillers (kaolinite and calcite) was observed. This shift reflects the degradation of the organic binder, confirmed by a reduction in the characteristic binder-related peaks. These findings suggest that the binder matrix undergoes significant photodegradation under visible light exposure, leading to a relative enrichment of inorganic filler signals, as previously reported [15,22].

According to the literature [35,36], the polymerization progress of a methacrylate (MA) resin can be monitored by tracking the unsaturation within the chain, specifically the C=C stretching at 1635 cm^{-1}. The ratio between the C=C (1635 cm^{-1}) and carbonyl peaks (Figure 7) increased over time, indicating chemical changes within the polymeric network of the binder. In PR112-containing paints, a moderate reduction in the binder-to-pigment ratio was also observed, suggesting that, while both components degrade, the binder is more affected under these conditions.

A similar behavior of FTIR band ratios was observed for orange paint mock-ups aged in a high relative humidity (RH) environment (see Supplementary Figure S2). However, for the PO5 pigment, a high variability in the binder-to-pigment ratio was observed at several monitoring points. Up to day 50, no substantial differences were detected between samples aged under high RH and those aged in ambient conditions. Although the degradation appears to be slightly more pronounced in an uncontrolled humidity environment, the high variability prevents us from drawing definitive conclusions. This observation aligns with the colorimetric results, which suggest a pigment-dependent influence of RH on the fading behavior.

Given the controlled laboratory conditions and the absence of mechanical stressors such as wind, rain, or particulate abrasion, erosion-related phenomena can be reasonably excluded as contributors to the observed degradation. Supplementary Figures S2–S4 provide a detailed spectral evolution over time, highlighting how RH conditions influence the degradation kinetics of both the binder and pigment components.

Micro Spatially Offset Raman Spectroscopy (micro-SORS) was employed to investigate depth-dependent compositional changes in artificially aged and unaged red paint mock-ups (Figure 8a). The advantage of this technique lies in its ability to obtain information non-invasively, avoiding the need for cross-sectional analysis. It also enables a more comprehensive study by allowing the investigation of multiple areas of the sample rather than being limited to a single cross-section. The recent development of micro-SORS in portable devices [50] also enables in situ studies, eliminating the need for sampling.

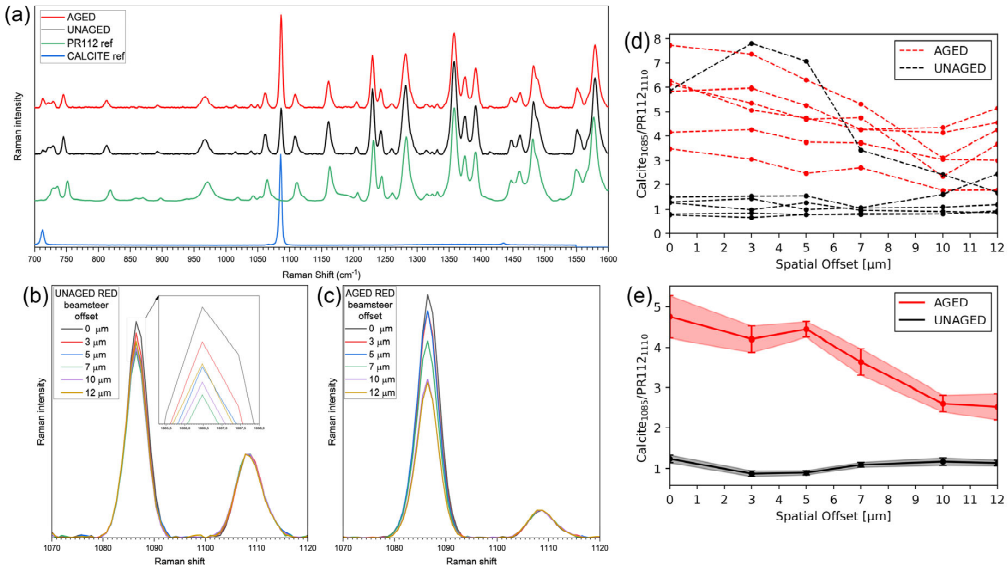

Figure 8. Raman and micro-SORS analyses on red paint mock-ups. (**a**) Raman spectra at a 0 spatial offset for unaged and aged mock-ups, along with reference spectra of the PR112 pigment and calcite [42,43]; (**b**,**c**) average Raman spectra at each offset values, collected from unaged (**b**) and aged (**c**) mockup, normalized at 1110 cm^{-1}; (**d**) ratio plot from individual micro-SORS series; and (**e**) average ratio plots with standard deviations for unaged and aged paints.

To assess the compositional changes, the symmetric stretching of C-O bonds in calcite (1085 cm^{-1}) [51] and a nearby peak attributed to the C-N symmetric stretching of the PR112 pigment (1110 cm^{-1}) [52,53] were analyzed. In unaged samples (Figure 8b), Raman signals of calcite and PR112 showed a random distribution across spatial offsets, likely due to the heterogeneous dispersion of the calcite agglomerates of crystals within the paint matrix. The absence of correlation between the signal intensity and spatial offsets (Figure 8d,e) confirms this distribution.

In contrast, aged samples (Figure 8c,e) exhibited a pronounced surface enrichment of calcite relative to the PR112, with the calcite signals decreasing monotonically with increasing depth (increasing offsets). The calcite/PR112 ratio, based on fitted peak heights, was lower and non-monotonic in unaged paints, consistent with the random distribution of both components. Micro-SORS, thus, non-invasively revealed that, in the aged mock-ups, calcite is concentrated towards the surface, while the pigment PR112 remains only in the deeper layer of the paint. Unfortunately, binder-related peaks could not be detected via Raman and micro-SORS spectroscopy. The depth resolution of micro-SORS cannot be reliably determined, as it depends on multiple factors, including the optical properties and heterogeneity of the materials, as well as the acquisition parameters. Thus, it has not been possible to associate specific depths within the material with the individual micro-SORS steps [54].

The results from pigment pellets (§3.1) and commercial paint mock-ups (§3.2) show that both the pigment and binder are affected by the VIS irradiation. Color fading is already evident in pigment pellets, as confirmed by the reduction in specific spectroscopic

signals attributed to SOPs. In paint mock-ups, degradation also affects the binder matrix, as evidenced by a progressive loss in FTIR bands associated with the polymer and a surface enrichment of inorganic fillers. This suggests that, in paint systems, binder photodegradation significantly contributes to pigment loss, likely through physical detachment and the increased exposure of pigment particles to light, thereby facilitating the degradation of the pigment itself. Other complementary mechanisms, such as oxidation at the pigment–binder interface and binder embrittlement, can be hypothesized as further promoting the pigment particles' detachment and the surface enrichment of inorganic fillers. These processes cannot be entirely ruled out, and further research is necessary in order to better disclose the exact degradation pathways.

The effect of relative humidity (RH) on color fading appears to be pigment-dependent: while a high RH accelerates fading for PR112 and PV23, it seems to slow it down for PY74 and PY83. This variability suggests that conservation strategies cannot rely on general rules but must consider the specific composition of the painting materials. In particular, RH control could be a useful tool with which to mitigate degradation in some cases, but could be potentially harmful in others. Further studies are needed in order to explore this interaction and define the optimal environmental protocols for the preservation of contemporary murals.

4. Conclusions

This study confirms that both synthetic organic pigments (SOPs) and acrylic–vinyl binders are susceptible to degradation under visible light exposure, with observable effects in both pigment pellets and commercial paint systems. In the former, color fading is attributed to the intrinsic photo instability of SOPs. In paint mock-ups, binder degradation was also evident and, in some cases, more pronounced than for pigments. Further experiments on pure pigments and the binder alone may help to confirm and better define the degradation mechanism of the paint system.

The influence of relative humidity (RH) on color fading emerged as pigment-dependent: high RH accelerated fading for some pigments (e.g., PR112 and PV23), while it mitigated it for others (e.g., PY74, PY83). This suggests that the chemical nature of the pigment plays a key role in modulating degradation under high humidity conditions. Although the hypothesis of the formation of volatile byproducts remains a plausible mechanism for paint degradation, the current data do not allow this to be fully confirmed. Further studies are needed to clarify the degradation pathways of SOPs and to support the development of conservation strategies tailored to the specific composition of modern paint systems.

Supplementary Materials: The supporting information can be downloaded at: https://www.mdpi.com/article/10.3390/app151810188/s1. Figure S1. Emission spectrum of the light employed in light aging; Figure S2. Evolution of ATR-FTIR bands' intensity ratios for red paint in uncontrolled relative humidity (DRY) aging environment at 0, 15, 30, 50, and 100 days of simulated days of exposure; Figure S3. Evolution of ATR-FTIR bands' intensity ratios for orange paint in high relative humidity (RH) aging environment at 0, 15, 30, 50, and 100 days of simulated days of exposure; Figure S4. Evolution of ATR-FTIR bands' intensity ratios for orange paint in in uncontrolled relative humidity (DRY) aging environment at 0, 15, 30, 50, and 100 days of simulated days of exposure; Table S1. Comparison of color difference values (ΔE) obtained from calibrated photographic images (ΔE_1) and VIS reflectance spectroscopy (ΔE_2) for various pigment and paint samples. The strong agreement between the two methods, confirmed by a Pearson correlation coefficient of 0.998, validates the use of calibrated image analysis as a reliable alternative for colorimetric evaluation in conservation studies.

Author Contributions: Conceptualization, N.G., C.C., S.G. and L.T.; methodology, N.G., C.C., S.G. and L.T.; software, K.A., N.G., M.P. and C.C.; validation, N.G., C.C., S.G. and L.T.; formal analysis,

N.G., C.C. and K.A.; investigation, N.G., C.C. and P.G.G.L.; data curation, N.G., C.C. and K.A.; writing—original draft preparation, N.G.; writing—review and editing, C.C., K.A., M.P., P.G.G.L., S.G. and L.T.; visualization, N.G., C.C., K.A., S.G. and L.T.; supervision, L.T., S.G. and M.P.; project administration, S.G. and L.T.; funding acquisition, S.G. and L.T. All authors have read and agreed to the published version of the manuscript.

Funding: P.G.G.L.'s PhD research was financially supported by the Italian PON "Ricerca e Innovazione" 2014–2020 funding program DOT1316197 (IMTR) CUP D45F21003710001 (Green).

Data Availability Statement: The raw data supporting the conclusions of this article will be made available by the authors upon request.

Acknowledgments: The authors would like to thank Ilaria Degano and Francesca Modugno (SCIBEC, University of Pisa) for performing the preliminary HPLC analyses and for their valuable suggestions during the preparation of the manuscript.

Conflicts of Interest: The authors declare no conflicts of interest.

Abbreviations

The following abbreviations are used in this manuscript:

SOPs	Synthetic Organic Pigments
SORS	Spatially Offset Raman Spectroscopy
FTIR	Fourier-Transform InfraRed
ATR	Attenuated Total Reflectance
PV	Pigment Violet
PR	Pigment Red
PY	Pigment Yellow
PO	Pigment Orange
DAC	Diamond Anvil Cell
PCA	Principal Component Analysis
MA	Methacrylate
UV	Ultraviolet
RH	Relative Humidity
CFL	Compact Fluorescent Lamp
HPLC-MS/MS	High-Performance Liquid Chromatography-coupled Tandem Mass Spectrometry

References

1. Pagnin, L.; Guarnieri, N.; Izzo, F.C.; Goidanich, S.; Toniolo, L. Protecting Street Art from Outdoor Environmental Threats: What Are the Challenges? *Coatings* **2023**, *13*, 2044. [CrossRef]
2. Groeneveld, I.; Kanelli, M.; Ariese, F.; van Bommel, M.R. Parameters That Affect the Photodegradation of Dyes and Pigments in Solution and on Substrate—An Overview. *Dye. Pigment.* **2023**, *210*, 110999. [CrossRef]
3. Mezzadri, P. Contemporary Murals in the Street and Urban Art Field: Critical Reflections between Preventive Conservation and Restoration of Public Art. *Heritage* **2021**, *4*, 2515–2525. [CrossRef]
4. Guarnieri, N.; Di Benedetto, A.; Comelli, D.; Mirani, F.; Dellasega, D.; Pagnin, L.; Goidanich, S.; Toniolo, L. Rapid Chromatic Alteration of Street Art: Mechanisms of Deterioration of the Painting Materials of the *20 Years of Freedom and Democracy* Mural. *Dye. Pigment.* **2025**, *239*, 112733. [CrossRef]
5. Alonso Villar, E.M.; Rivas Brea, M.T.; Pozo Antonio, J.S. Resistance to Artificial Daylight of Paints Used in Urban Artworks. Influence of Paint Composition and Substrate. *Prog. Org. Coat.* **2021**, *154*, 106180. [CrossRef]
6. Anghelone, M.; Jembrih-Simbürger, D.; Pintus, V.; Schreiner, M. Photostability and Influence of Phthalocyanine Pigments on the Photodegradation of Acrylic Paints under Accelerated Solar Radiation. *Polym. Degrad. Stab.* **2017**, *146*, 13–23. [CrossRef]
7. Marazioti, V.; Douvas, A.M.; Vouvoudi, E.C.; Bikiaris, D.; Papadokostaki, K.; Nioras, D.; Gogolides, E.; Orfanoudakis, S.; Stergiopoulos, T.; Boyatzis, S.; et al. The Condition of Contemporary Murals in Sun-Exposed Urban Environments: A Model Study Based on Spray-Painted Mock-Ups and Simulated Light Ageing. *Heritage* **2024**, *7*, 3932–3959. [CrossRef]

8. Doménech-Carbó, M.T.; Silva, M.F.; Aura-Castro, E.; Fuster-López, L.; Kröner, S.; Martínez-Bazán, M.L.; Más-Barberá, X.; Mecklenburg, M.F.; Osete-Cortina, L.; Doménech, A.; et al. Study of Behaviour on Simulated Daylight Ageing of Artists' Acrylic and Poly(Vinyl Acetate) Paint Films. *Anal. Bioanal. Chem.* **2011**, *399*, 2921–2937. [CrossRef] [PubMed]
9. Cimino, D.; Lamuraglia, R.; Saccani, I.; Berzioli, M.; Izzo, F.C. Assessing the (In)Stability of Urban Art Paints: From Real Case Studies to Laboratory Investigations of Degradation Processes and Preservation Possibilities. *Heritage* **2022**, *5*, 581–609. [CrossRef]
10. Sabatini, F.; La Nasa, J.; Degano, I.; Campanella, B.; Legnaioli, S.; Saccani, I.; Modugno, F. Fluorescent Paints in Contemporary Murals: A Case Study. *Heritage* **2023**, *6*, 5689–5699. [CrossRef]
11. Rivas, T.; Alonso-Villar, E.M.; Pozo-Antonio, J.S. Forms and Factors of Deterioration of Urban Art Murals under Humid Temperate Climate; Influence of Environment and Material Properties. *Eur. Phys. J. Plus* **2022**, *137*, 1257. [CrossRef]
12. Pozo-Antonio, J.S.; Alonso-Villar, E.M.; Rivas, T.; Márquez, I. Evaluation of a Protective Acrylic Finish Applied to Surfaces Painted with Acrylic Paints for Outdoor or Indoor Uses. *Dye. Pigment.* **2023**, *212*, 111141. [CrossRef]
13. Magrini, D.; Bracci, S.; Cantisani, E.; Conti, C.; Rava, A.; Sansonetti, A.; Shank, W.; Colombini, M. A Multi-Analytical Approach for the Characterization of Wall Painting Materials on Contemporary Buildings. *Spectrochim. Acta Part A Mol. Biomol. Spectrosc.* **2017**, *173*, 39–45. [CrossRef]
14. Batchelor, S.N.; Carr, D.; Coleman, C.E.; Fairclough, L.; Jarvis, A. The Photofading Mechanism of Commercial Reactive Dyes on Cotton. *Dye. Pigment.* **2003**, *59*, 269–275. [CrossRef]
15. Anghelone, M.; Stoytschew, V.; Jembrih-Simbürger, D.; Schreiner, M. Spectroscopic Methods for the Identification and Photostability Study of Red Synthetic Organic Pigments in Alkyd and Acrylic Paints. *Microchem. J.* **2018**, *139*, 155–163. [CrossRef]
16. Anghelone, M.; Jembrih-Simbürger, D.; Schreiner, M. Influence of Phthalocyanine Pigments on the Photo-Degradation of Alkyd Artists' Paints under Different Conditions of Artificial Solar Radiation. *Polym. Degrad. Stab.* **2016**, *134*, 157–168. [CrossRef]
17. Ciccola, A.; Guiso, M.; Domenici, F.; Sciubba, F.; Bianco, A. Azo-Pigments Effect on UV Degradation of Contemporary Art Pictorial Film: A FTIR-NMR Combination Study. *Polym. Degrad. Stab.* **2017**, *140*, 74–83. [CrossRef]
18. La Nasa, J.; Campanella, B.; Sabatini, F.; Rava, A.; Shank, W.; Lucero-Gomez, P.; De Luca, D.; Legnaioli, S.; Palleschi, V.; Colombini, M.P.; et al. 60 Years of Street Art: A Comparative Study of the Artists' Materials through Spectroscopic and Mass Spectrometric Approaches. *J. Cult. Herit.* **2021**, *48*, 129–140. [CrossRef]
19. Krmpotić, M.; Jembrih-Simbürger, D.; Siketić, Z.; Marković, N.; Anghelone, M.; Tadić, T.; Plavčić, D.; Malloy, M.; Radović, I.B. Identification of Synthetic Organic Pigments (SOPs) Used in Modern Artist's Paints with Secondary Ion Mass Spectrometry with MeV Ions. *Anal. Chem.* **2020**, *92*, 9287–9294. [CrossRef] [PubMed]
20. Bosi, A.; Ciccola, A.; Serafini, I.; Guiso, M.; Ripanti, F.; Postorino, P.; Curini, R.; Bianco, A. Street Art Graffiti: Discovering Their Composition and Alteration by FTIR and Micro-Raman Spectroscopy. *Spectrochim. Acta Part A Mol. Biomol. Spectrosc.* **2020**, *225*, 117474. [CrossRef]
21. Marazioti, V.; Douvas, A.M.; Katsaros, F.; Koralli, P.; Chochos, C.; Gregoriou, V.G.; Boyatzis, S.; Facorellis, Y. Chemical Characterisation of Artists' Spray-Paints: A Diagnostic Tool for Urban Art Conservation. *Spectrochim. Acta Part A Mol. Biomol. Spectrosc.* **2023**, *291*, 122375. [CrossRef]
22. Rousaki, A.; Vandenabeele, P.; Berzioli, M.; Saccani, I.; Fornasini, L.; Bersani, D. An In-and-out-the-Lab Raman Spectroscopy Study on Street Art Murals from Reggio Emilia in Italy. *Eur. Phys. J. Plus* **2022**, *137*, 252. [CrossRef]
23. Sabatini, F.; Albertin, F.; Doherty, B.; Monico, L.; Rosi, F.; Buti, D.; Romani, A.; Pecci, A.; Abate, N.; Sileo, M.; et al. Unveiling Street Art: A Multimodal and Multitechnique Approach for Analyzing and Mapping Painting Materials on Large Murals. *Proc. Natl. Acad. Sci. USA* **2025**, *122*, e2504918122. [CrossRef] [PubMed]
24. Guarnieri, N.; Pagnin, L.; Berti, L.; Goidanich, S.; Gulotta, D.; Izzo, F.C.; Toniolo, L. Preserving the Contemporary Mural "Musica Popolare" by Orticanoodles in Milan, Italy: Deterioration Processes and Protection Performance of Commercial Coatings. *J. Cult. Herit.* **2025**, *75*, 326–332. [CrossRef]
25. Pellis, G.; Bertasa, M.; Ricci, C.; Scarcella, A.; Croveri, P.; Poli, T.; Scalarone, D. A Multi-Analytical Approach for Precise Identification of Alkyd Spray Paints and for a Better Understanding of Their Ageing Behaviour in Graffiti and Urban Artworks. *J. Anal. Appl. Pyrolysis* **2022**, *165*, 105576. [CrossRef]
26. Ghelardi, E.; Degano, I.; Colombini, M.P.; Mazurek, J.; Schilling, M.; Khanjian, H.; Learner, T. A Multi-Analytical Study on the Photochemical Degradation of Synthetic Organic Pigments. *Dye. Pigment.* **2015**, *123*, 396–403. [CrossRef]
27. Papliaka, Z.E.; Andrikopoulos, K.S.; Varella, E.A. Study of the Stability of a Series of Synthetic Colorants Applied with Styrene-Acrylic Copolymer, Widely Used in Contemporary Paintings, Concerning the Effects of Accelerated Ageing. *J. Cult. Herit.* **2010**, *11*, 381–391. [CrossRef]
28. Winston, P.W.; Bates, D.H. Saturated Solutions For the Control of Humidity in Biological Research. *Ecology* **1960**, *41*, 232–237. [CrossRef]
29. ENEA (Agenzia Nazionale per le Nuove Tecnologie, L'energia e lo Sviluppo Economico Sostenibile) Atlante Italiano Della Radiazione Solare. Available online: https://www.solaritaly.enea.it/CalcRggmmNorm/Calcola3.php (accessed on 1 March 2025).

30. Guan, L.; Berrill, T.; Brown, R.J. Measurement of Actual Efficacy of Compact Fluorescent Lamps (CFLs). *Energy Build.* **2015**, *86*, 601–607. [CrossRef]
31. *EN ISO/CIE 11664-4:2019*; Colorimetry—Part 4: CIE 1976 L*a*b* Colour Space. International Organization for Standardization: Geneva, Switzerland, 2019.
32. *UNI EN 15886:2010*; Conservation of Cultural Property—Test Methods—Colour Measurements of Surfaces. European Committee for Standardization: Brussels, Belgium, 2010.
33. Chércoles Asensio, R.; San Andrés Moya, M.; de la Roja, J.M.; Gómez, M. Analytical Characterization of Polymers Used in Conservation and Restoration by ATR-FTIR Spectroscopy. *Anal. Bioanal. Chem.* **2009**, *395*, 2081–2096. [CrossRef]
34. Pintus, V.; Wei, S.; Schreiner, M. Accelerated UV Ageing Studies of Acrylic, Alkyd, and Polyvinyl Acetate Paints: Influence of Inorganic Pigments. *Microchem. J.* **2016**, *124*, 949–961. [CrossRef]
35. Fu, J.; Liu, W.; Hao, Z.; Wu, X.; Yin, J.; Panjiyar, A.; Liu, X.; Shen, J.; Wang, H. Characterization of a Low Shrinkage Dental Composite Containing Bismethylene Spiroorthocarbonate Expanding Monomer. *Int. J. Mol. Sci.* **2014**, *15*, 2400–2412. [CrossRef] [PubMed]
36. Delgado, A.H.; Young, A.M. Modelling ATR-FTIR Spectra of Dental Bonding Systems to Investigate Composition and Polymerisation Kinetics. *Materials* **2021**, *14*, 760. [CrossRef]
37. Mooney, E.F. The Infrared Spectra of Chlorobenzene and Bromobenzene Derivatives—III. Toluenes. *Spectrochim. Acta* **1964**, *20*, 1343–1348. [CrossRef]
38. Wang, X.; He, X.; Wang, X. FTIR Analysis of the Functional Group Composition of Coal Tar Residue Extracts and Extractive Residues. *Appl. Sci.* **2023**, *13*, 5162. [CrossRef]
39. Pagnin, L.; Calvini, R.; Wiesinger, R.; Weber, J.; Schreiner, M. Photodegradation Kinetics of Alkyd Paints: The Influence of Varying Amounts of Inorganic Pigments on the Stability of the Synthetic Binder. *Front. Mater.* **2020**, *7*, 600887. [CrossRef]
40. Vieira, M.; Melo, M.J.; Conti, C.; Pozzi, F. A Combined Approach to the Vibrational Characterization of Medieval Paints on Parchment: Handheld Raman Spectroscopy and Micro-SORS. *J. Raman Spectrosc.* **2024**, *55*, 263–275. [CrossRef]
41. Botteon, A.; Kim, W.-H.; Colombo, C.; Realini, M.; Castiglioni, C.; Matousek, P.; Kim, B.-M.; Kwon, T.-H.; Conti, C. Non-Destructive Monitoring of Dye Depth Profile in Mesoporous TiO_2 Electrodes of Solar Cells with Micro-SORS. *Anal. Chem.* **2022**, *94*, 2966–2972. [CrossRef] [PubMed]
42. RMP00052, Calcium Carbonate, Reference Collections, Museum of Fine Arts, Boston | IRUG Library. Available online: http://irug.org/jcamp-details?id=3484 (accessed on 25 August 2025).
43. ROD00563, Pigment Red 112 (PR112), Naphthol AS, CI12370, Royal Institute for Cultural Heritage (KIK/IRPA), IRUG Library. Available online: http://irug.org/jcamp-details?id=6622 (accessed on 25 August 2025).
44. Scherrer, N.C.; Stefan, Z.; Francoise, D.; Annette, F.; Renate, K. Synthetic Organic Pigments of the 20th and 21st Century Relevant to Artist's Paints: Raman Spectra Reference Collection. *Spectrochim. Acta. A. Mol. Biomol. Spectrosc.* **2009**, *73*, 505–524. [CrossRef]
45. Salomon, R. Evolutionary Algorithms and Gradient Search: Similarities and Differences. *IEEE Trans. Evol. Comput.* **1998**, *2*, 45–55. [CrossRef]
46. IOD00367, Pigment Red 112 (PR112), Naphthol AS, Azo, CI12370, Interactive, PMA, IRUG Spectrum Database. Available online: http://irug.org/jcamp-details?id=568 (accessed on 27 May 2025).
47. IMP00108, Calcium Carbonate, Anhydrous Normal Carbonate, CaCO2, PMA, Interactive IRUG Spectrum Database. Available online: http://irug.org/jcamp-details?id=463 (accessed on 27 May 2025).
48. IMP00024, Gypsum (Ca(SO4)*2H2O), GCI, Interactive IRUG Spectrum Database. Available online: http://irug.org/jcamp-details?id=220 (accessed on 27 May 2025).
49. ROD00393, Pigment Violet 23 (PV23), Dioxazine, Polycyclic, CI51319, Royal Institute for Cultural Heritage, KIK/IRPA, IRUG Database. Available online: http://www.irug.org/jcamp-details?id=6416 (accessed on 27 August 2025).
50. Lux, A.; Realini, M.; Botteon, A.; Maiwald, M.; Müller, A.; Sumpf, B.; Miliani, C.; Matousek, P.; Strobbia, P.; Conti, C. Advanced Portable Micro-SORS Prototype Coupled with SERDS for Heritage Science. *Analyst* **2024**, *149*, 2317–2327. [CrossRef] [PubMed]
51. Alves, J.F.; Edwards, H.G.M.; Korsakov, A.; de Oliveira, L.F.C. Revisiting the Raman Spectra of Carbonate Minerals. *Minerals* **2023**, *13*, 1358. [CrossRef]
52. Germinario, G.; van der Werf, I.D.; Sabbatini, L. Chemical Characterisation of Spray Paints by a Multi-Analytical (Py/GC–MS, FTIR, μ-Raman) Approach. *Microchem. J.* **2016**, *124*, 929–939. [CrossRef]
53. Vandenabeele, P.; Moens, L.; Edwards, H.G.M.; Dams, R. Raman Spectroscopic Database of Azo Pigments and Application to Modern Art Studies. *J. Raman Spectrosc.* **2000**, *31*, 509–517. [CrossRef]
54. Mosca, S.; Conti, C.; Stone, N.; Matousek, P. Spatially Offset Raman Spectroscopy. *Nat. Rev. Methods Primers* **2021**, *1*, 21. [CrossRef]